

Light output improvement of 10 W operated vertical LEDs via surface roughening using a commercialized developer

Tak Jeong · Hyung-Jo Park · Ki Chang Jung ·
Jong Hyeob Baek · Jun-Seok Ha · Won-Sik Choi ·
Si-Hyun Park

Received: 11 October 2014 / Accepted: 15 February 2015 / Published online: 25 February 2015
© The Author(s) 2015. This article is published with open access at Springerlink.com

Abstract We report improvement of improvement effectiveness of the light extraction efficiency of 10 W operated InGaN-based vertical light-emitting diodes via n-GaN surface roughening, using a *commercial photoresist (PR) developer* as an etching solution, which was compared with a conventional KOH-based solution. With the conventional KOH-based solution for n-GaN surface roughening, although both the depth and density of the etch pyramid initially increased with etching time, the depth eventually decreased and the density also decreased gradually, resulting in degradation in improvement effectiveness of extraction efficiency. Using the commercial PR developer for etching, however, after an initial increase in both the depth of the etch pyramid and its density, the depth and density were maintained without degradation, confirming the improvement in improvement effectiveness of extraction efficiency as well as the improvement in run to run fabrication uniformity. This may be due that with developer the GaN surface is etched only along the dislocation and is not etched over the non-defect region even as etching time goes on.

1 Introduction

Light-emitting diodes (LEDs) have many advantages as light sources, such as high-energy efficiency, long lifetimes, small size, excellent color rendering, and coverage of the entire optical spectrum from infrared (IR) to ultraviolet (UV). Various applications include indoor/outdoor general lighting, backlighting for liquid-crystal displays, automobile lighting, visible-light communications, and sterilization. LED efficiency, an important issue for all of the applications mentioned, can be divided into the following sub-efficiency categories: internal quantum efficiency, extraction efficiency, external quantum efficiency, wall-plug efficiency, and luminous efficiency. The internal quantum efficiency is defined as the ratio of the number of photons from the active region to the number of electrons injected into the LED. The extraction efficiency is defined as the ratio of the number of photons in free space to the number of photons from the active region. The external quantum efficiency is defined as the ratio of the number of photons in free space to the number of electrons injected into the LED; thus, the external quantum efficiency is equal to the product of the internal quantum efficiency and the extraction efficiency. The wall-plug efficiency is defined as the ratio of optical power out to electrical power in, and is therefore equal to the external quantum efficiency multiplied by the ratio of the photon energy to the electron energy. Finally, the luminous efficiency is defined as the ratio of luminous flux out to the electrical power in, and is therefore equal to the wall-plug efficiency multiplied by the standard luminous flux per optical power.

With regard to the extraction efficiency, the semiconductor material has a high refractive index; thus, some of the light generated inside the semiconductor cannot escape to the outside due total internal reflection at the interface. A

T. Jeong · H.-J. Park · K. C. Jung · J. H. Baek · W.-S. Choi
LED Device Research Center, Korea Photonics Technology
Institute, Gwangju 500-779, Republic of Korea

J.-S. Ha
Department of Applied Chemical Engineering, Chonnam
National University, Gwangju 500-757, Republic of Korea

W.-S. Choi · S.-H. Park (✉)
Department of Electronic Engineering, Yeungnam University,
280 Daehak-ro, Gyeongsan-si, Gyeongsangbuk-do 712-749,
Republic of Korea
e-mail: sihyun_park@ynu.ac.kr

simple rectangular-structured LED of InGaN-based material (refractive index: 2.5) is estimated to have an extraction efficiency of only 4 % [1], which is extremely small. Numerous studies have investigated methods of improving the extraction efficiency in LEDs, including chip shaping [2], flip-chip packaging [3], patterned sapphire substrates [4–7], resonant cavities [8], photonic crystal structures [9], surface plasmon coupling [10, 11], and surface roughening [12–31].

The surface roughening method is used to minimize the total internal reflection of the LED material through artificial roughening of the semiconductor's surface. This method is used widely due to its relatively simple fabrication process and improved extraction efficiency. Various approaches have been used to roughen the surface of InGaN-based LEDs, which are actually considered as one of the most popular among the various material-based LEDs in view of various device applications. With a conventional planar-type LED, the top p-GaN surface can be roughened [12–21] and (or) the n-GaN surface can also be roughened using a double-transfer technique for the wafer [22–24]. An additional layer, such as ZnO [25] or ITO [26], can be added to p-GaN and then roughened. With a vertical-type LED, the n-(or undoped) GaN surface can be roughened or patterned, after the substrate separation process [27–32]. While the roughening of the surface can be processed using several different methods, including wet-etching [12–14, 27, 28], dry-etching [15–17, 29], laser treatment [18, 19, 31], or control over the growth conditions [20, 21, 32], the wet-etching is commonly used, due to its low cost and simple experimental procedure. A KOH based-solution is one of the more widely used etchants for the wet-etching technique [33].

In this study, a commercial PR developer was suggested to be used for n-GaN surface roughening, and showed the improvement of improvement effectiveness of the light extraction efficiency of 10 W operated InGaN-based vertical LEDs with it, in comparison with the conventional KOH-based solution, in addition to the improvement in run to run fabrication uniformity. The detail etching mechanisms of InGaN surface etching was provided to explain the enhanced effects with the PR developer.

2 Experimental

Figure 1 shows scanning electron microscopy (SEM) images of N-face n-GaN surfaces etched using the conventional KOH etchant, for several etching times. A 5 mol KOH solution and an etching temperature of 80 °C were used for each case shown. Hexagonal pyramid-like patterns were observed over the entire n-GaN surface as a result of etching [27]. The height of the hexagonal pyramid

increased with the etching time up to ~10 min, as shown in Sample #4, upon which a maximum height of ~1.6 μm was achieved; however, the height decreased as the etching time increased beyond 10 min. The insets in Fig. 1 show the density of the etch pyramid in views with zoom-out scale. The density of hexagonal pyramids appeared to increase initially with the etching time up to ~3 min 40 s, as shown in Sample #3, but subsequently decreased with additional etching time. Here we prepared our samples with focusing on showing the etch trend with the variation of the pyramid height with constant interval. Therefore SEM pictures are with the pyramid heights of 0.4 μm in #1, 0.8 μm in #2, 1.2 μm in #3, 1.6 μm in #4, 1.0 μm in #5, and 0.5 μm in #6, respectively. For the sample with etch duration between #3 and #4 (it is not shown here), 6 min KOH etching duration resulted in the sample with the pyramid height of ~1.3 μm and the pyramid density of the decreased value in comparison with #3.

Figure 2 shows, on the other hand, SEM images of the N-face of n-GaN surfaces etched by the commercial PR developer (AZ300MIF, AZ Electronics Materials Corp., USA) for several etching times. Etching was conducted at 60 °C. The height of the hexagonal pyramids increased slowly with the etching time up to 110 min; Sample #5 shows the maximum height. Additional etching (beyond 110 min) did not affect the height of the pyramids (i.e., no additional change was observed), as shown in Sample #6. The density of the pyramids reached a maximum after 35 min of etching, as shown in Sample #2, and remained relatively unchanged with additional etching time.

We measured the total GaN thickness remaining of the sample after etching, d . The initial total GaN thickness before etching was 5 μm. Table 1 shows the measured result for d , accompanying the pyramid height or etched height, h . (See Fig. 5 for the definition of d and h in the sample) We can see the total GaN thickness remaining after etching decreased with etching time by KOH etching and it finally became same with the pyramid height, h . By developer etching, on the other hand, the total GaN thickness remaining after etching remained as a constant value (~5 μm) while the pyramid height, h increased initially and then was saturated, indicating no further more etching.

We fabricated InGaN-based vertical-type LED chips to compare the output power of the LED surface-roughened by the PR developer to that created by etching with a KOH-based solution. The epitaxial layer was prepared on a c-plane sapphire substrate by metal-organic chemical vapor deposition (MOCVD), and consisted of an n-GaN layer with the thickness of 5 μm, InGaN/GaN multiple quantum-well (MQW) active layers, an AlGaN electron-blocking layer (EBL), and a p-GaN layer. Using wafer bonding and the laser lift-off process, the vertical LED chip with the

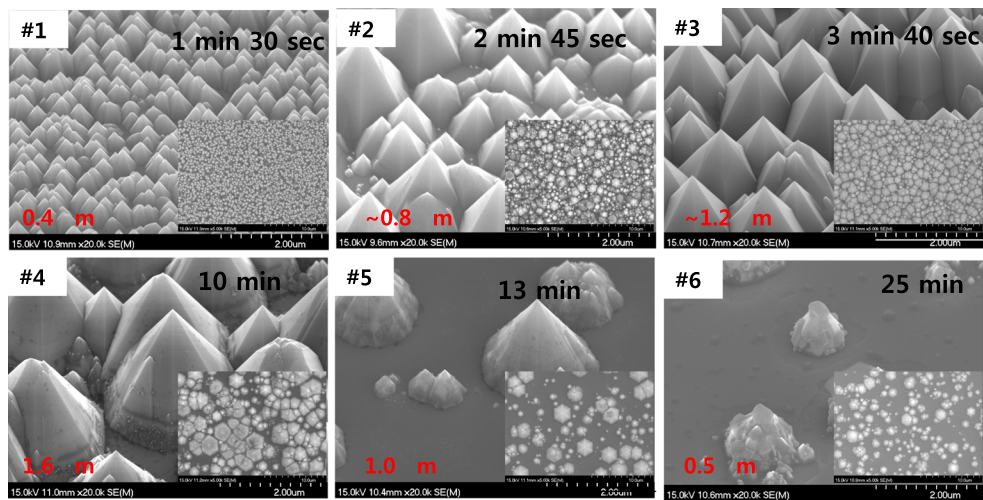


Fig. 1 Scanning electron microscopy (SEM) images of the N-face n-GaN surface etched with a conventional KOH etchant solution, for several etching times. The etching time and the height of the

hexagonal cones resulting from etching are indicated. The *inset* shows the etch pyramid density in views with zoom-out scale

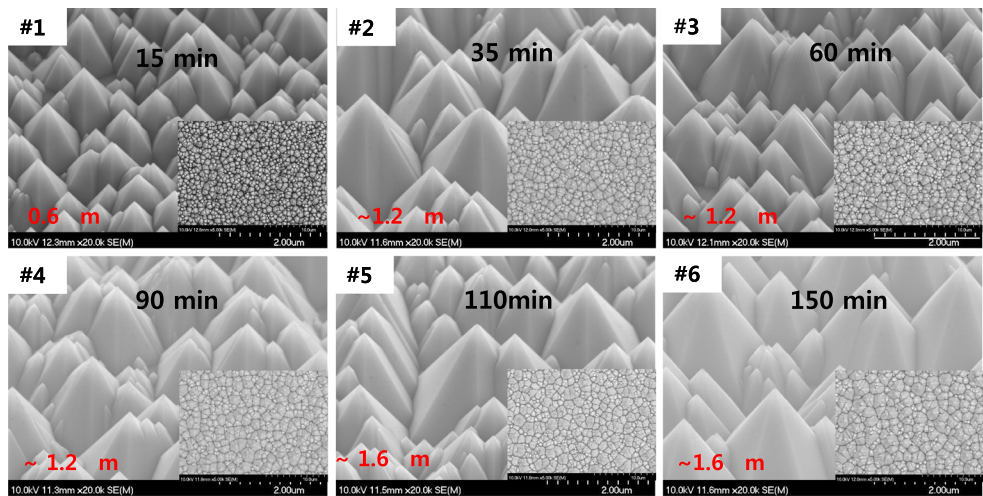


Fig. 2 SEM images of the N-face n-GaN surface etched by a commercial photoresist (PR) developer (AZ300MIF, AZ Electronics Materials Corp., USA)

Table 1 The pyramid height or etched height, h and the total GaN thickness remaining, d , after etching for each sample in Figs. 1 and 2

Sample #	#1	#2	#3	#4	#5	#6
h in KOH etching	~0.4	~0.8	~1.2	~1.6	~1.0	~0.5
d in KOH etching	~5	~4	~3.5	~2.5	~1.5	~0.5
h in developer etching	~0.6	~1.2	~1.2	~1.2	~1.6	~1.6
d in developer etching	~5	~5	~5	~5	~5	~5

unit: μm

N-face n-GaN surface as the surface top was prepared. The size of the individual chips was $1.8 \times 1.8 \text{ mm}^2$. The N-face n-GaN surface was roughened to the various etching conditions shown in Figs. 1 and 2 using the PR

developer or KOH solution. The same GaN LED wafer was used for the comparison etch test. We mounted each LED chip in a ceramic package and encapsulated it with epoxy resin. Then we placed the PKG LED on a thermal stage. In

order to examine its operation properties, each chip was operated under the pulsed current injection with a pulse width of 1 ms and a duty cycle of 0.1 %, minimizing a heating effect. Figure 3 shows output power under the input current level of 2 A for all samples in Figs. 1 and 2, from Sample #1 to #6 with KOH and the developer.

It is a common notion that the pyramid density is indeed an important key factor while the pyramid height is not a major one as long as it is higher than a certain critical value. To state it differently, the pyramid height must be higher than the certain critical value in order for keeping the high light extraction efficiency. This critical value seems to be at least 1.5 μm from our experimental results. For the samples roughened with KOH, the output power increased rapidly until at Sample #3, which may be contributed to both the increment of the pyramid density and the increment of the pyramid height. In the time zone between Sample #3 and Sample #4, however, the output power seemed to remain relatively unchanged which may be contributed to two conflicting effects, i.e., the slight decrease in the pyramid density and the increase in the pyramid height to 1.6 μm . Therefore the pyramid height still contributed to the increase of the extraction efficiency until this height reached the critical value. After Sample #4, there was the rapid decrease in the output power, which may be considered to be mainly due to the decrease in the pyramid density. For the samples roughened with the developer, the output power increased rapidly until at Sample #2, which may be contributed to both the increment of the pyramid density and the increment of the pyramid height. However, the rate of the increment of the output power was down after Sample #2, showing the relatively slow increase in the output power until Sample #5, and then it seemed to be zero after Sample #5, showing no increment in the output power. That shows clearly that the effect of the

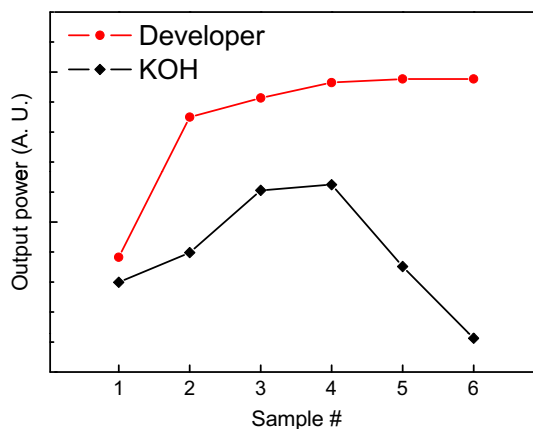


Fig. 3 Output power at the input current level of 2 A for all InGaN-based vertical-type LEDs with n-GaN surface roughening shown in Figs. 1 and 2, from Sample #1 to #6 with KOH and the developer

height of the pyramids becomes negligible after the certain height (over 1.5 μm in our case). In comparison of the inset of #3 of Fig. 1 and that of #2 of Fig. 2, we can observe that there is a considerable portion of void over a whole wafer in #3 of Fig. 1 and therefore that the pyramid density in #2 of Fig. 2 is higher than that in #3 of Fig. 1, resulting in ample differences in their extraction efficiency in Fig. 3. About the concern related with concentration of KOH etchant, we observed that a dilute KOH etchant for the etching process made no difference in these phenomenon characteristics, but a difference only in an etching rate or equivalently an etching time.

To sum up, the certain critical value of the pyramid height can be reached by KOH etching. The pyramid density, however, was drastically decreased with the etching time by KOH etching, resulting in decreasing the light output power. On the other hand, the surface state with the pyramid height of over 1.5 μm can have the maximum value of the pyramid density simultaneously by developer etching, resulting in producing higher output power of LEDs.

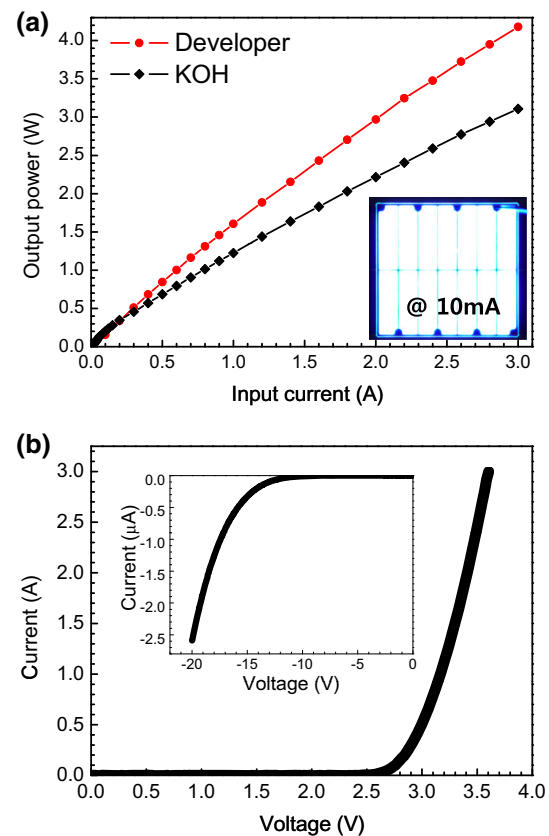
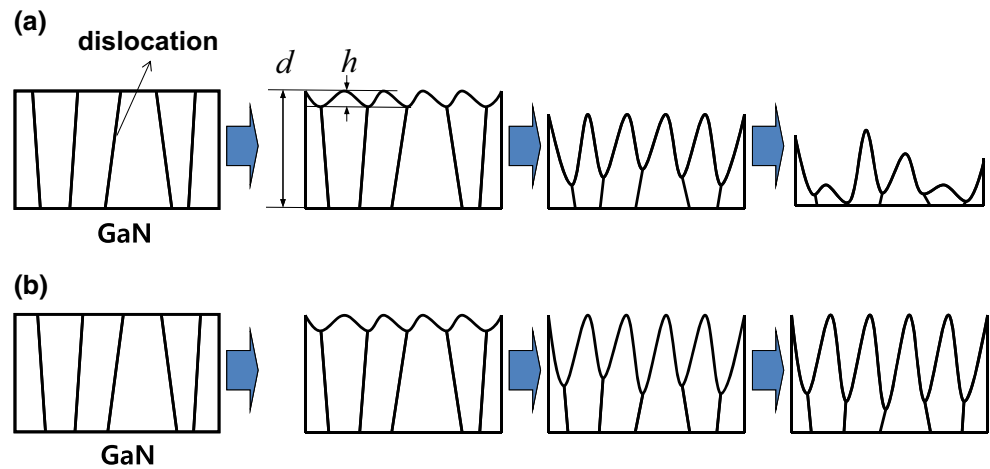


Fig. 4 **a** Output power as a function of the input current for the samples with maximum output power in Fig. 3, that is, Sample #4 with KOH and Sample #5 with the developer. The inset shows an emission image of the chip (size: 1.8 \times 1.8 mm^2) at a 10-mA input for Sample #5 with the developer. **b** Current versus voltage graph

Fig. 5 GaN etching mechanism using **a** a conventional etchant (KOH), and **b** a commercial PR developer



We also measured output power as a function of the input current for the samples with maximum output power in Fig. 3, that is, Sample #4 with KOH and Sample #5 with the developer, which is shown in Fig. 4a. The LED etched by the developer and KOH solution produced output powers of 4.12 W and 3.11 W, respectively, for an input current of 3 A, corresponding to a 34.5 % enhancement in the improvement effectiveness of the extraction efficiency for the LED etched by the developer. In I–V curve of (b), there was little difference between two samples indicating no difference in electronics properties resulted from different etching solutions.

It was reported that the formation of etch pits during etch of Ga-face GaN surface is on the dislocation sites [34] and it was also reported that the density of the protruding etch features during etch of N-face GaN surface correlates with the density of dislocations established from cross-sectional TEM investigation of the same material [35]. From the above reported results, Table 1 as well as SEM photos of Figs. 1 and 2 have naturally led us to the schematic diagram of Fig. 5 for the etching process, following the proposal of possible etching mechanism. With KOH, the GaN surface is *initially* etched along the dislocation [34, 35]. As etching time goes on, however, it become to be etched over the whole GaN surface including the non-defect region. As a result, the pyramid density starts to decrease after a certain etching time. With developer, however, the GaN surface is etched only along the dislocation. The GaN surface is not etched over the non-defect region even as etching time goes on. As a result, the pyramid density is continuously kept after a certain etching time.

3 Conclusions

A commercial PR developer was used as the etching solution for n-GaN surface roughening in a vertical-type LED chip with $1.8 \times 1.8 \text{ mm}^2$ area. The LED extraction

efficiency improved by 34.5 % in $\sim 10 \text{ W}$ operations, in comparison with that of an LED etched with a conventional KOH-based solution, showing the output power of 4.12 W. For the n-GaN surface etched by the commercial PR developer, the two key parameters for the enhancement of the LED extraction efficiency, the etch pyramid height and the density of pyramids, increased initially and then became saturated over time, without degradation or decrease in function. Thus, the optimization of these two key parameters may occur simultaneously after a certain etching time has elapsed, enhancing the extraction efficiency of the LED, and improving the stability in run-to-run process uniformity. These results were attributed to that the GaN surface using developer is etched only along the dislocation and not etched over the non-defect region even as etching time goes on.

Acknowledgments This work was supported in part by the National IT Industry Promotion Program of the Ministry of Science, ICT and Future Planning, Korea, under Grant I2201-14-1002.

Open Access This article is distributed under the terms of the Creative Commons Attribution License which permits any use, distribution, and reproduction in any medium, provided the original author(s) and the source are credited.

References

1. E.F. Schubert, *Light-Emitting Diodes*, 2nd edn. (Cambridge Univ. Press, Cambridge, 2006)
2. S.E. Brinkley, C.L. Keraly, J. Sonoda, C. Weisbuch, J.S. Speck, S. Nakamura, S.P. Denbaars, *Appl. Phys. Express* **5**, 032104 (2012)
3. J.J. Wierer, D.A. Steigerwald, M.R. Krames, J.J. O'Shea, M.J. Ludowise, G. Christenson, Y.C. Shen, C. Lowery, P.S. Martin, S. Subramanya, W. Gotz, N.F. Gardner, R.S. Kern, S.A. Stockman, *Appl. Phys. Lett.* **78**, 3379 (2001)
4. X.-H. Huang, J.-P. Liu, J.-J. Kong, H. Yang, H.-B. Wang, *Opt. Express* **19**, A949 (2011)
5. J.H. Lee, J.T. Oh, Y.C. Kim, J.H. Lee, *IEEE Photonics Technol. Lett.* **20**, 1563 (2008)

6. Y.K. Su, J.J. Chen, C.L. Lin, S.M. Chen, W.L. Li, C.C. Kao, J. Cryst. Growth **311**, 2973 (2009)
7. Y.T. Hsu, C.C. Yu, K.F. Huang, W.H. Lan, J.E. Huang, J.C. Lin, W.J. Lin, IEEE Photonics Technol. Lett. **24**, 1686 (2012)
8. D. Delbeke, R. Bockstaele, P. Bienstman, R. Baets, H. Benisty, IEEE J. Sel. Top. Quantum Electron. **8**, 189 (2002)
9. D.H. Kim, C.O. Cho, Y.G. Roh, H.S. Jeon, Y.S. Park, J.H. Cho, J.S. Im, C.S. Sone, Y.J. Park, W.J. Choi, Q.H. Park, Appl. Phys. Lett. **87**, 203508 (2005)
10. W.L. Barnes, J. Lightwave Technol. **17**, 2170 (1999)
11. J. Vuckovic, M. Loncar, A. Scherer, IEEE J. Quantum Electron. **36**, 1131 (2000)
12. C. Huh, K.-S. Lee, E.-J. Kang, S.-J. Park, J. Appl. Phys. **93**, 9383 (2003)
13. H.-Y. Lee, X.-Y. Huang, C.-T. Lee, J. Electrochem. Soc. **155**, H707 (2008)
14. A.C. Tamboli, K.C. McGroddy, E.L. Hu, Phys. Status Solidi C **6**, S807 (2009)
15. K. Kim, J. Choi, T.S. Baw, M. Jung, D.H. Woo, Jpn. J. Appl. Phys. **46**, 6682 (2007)
16. M.-Y. Hsieh, C.-Y. Wang, L.-Y. Chen, T.-P. Lin, M.-Y. Ke, Y.-W. Cheng, Y.-C. Yu, C.P. Chen, D.-M. Yeh, C.-F. Lu, C.-F. Huang, C.C. Yang, J.J. Huang, IEEE Electron Device Lett. **29**, 658 (2008)
17. T. Wei, Q. Kong, J. Wang, J. Li, Y. Zeng, G. Wang, J. Li, Y. Liao, F. Yi, Opt. Express **19**, 1065 (2011)
18. H.-W. Huang, J.T. Chu, C.C. Kao, T.H. Hseuh, T.C. Lu, H.C. Kuo, S.C. Wang, C.C. Yu, Nanotechnology **16**, 1844 (2005)
19. H.-W. Huang, C.C. Kao, J.T. Chu, W.D. Liang, H.C. Kuo, S.C. Wang, C.C. Yu, Mater. Chem. Phys. **99**, 414 (2006)
20. C.H. Kuo, C.W. Kuo, C.M. Chen, B.J. Pong, G.C. Chi, Appl. Phys. Lett. **89**, 191112 (2006)
21. X.-J. Zhuo, J. Zhang, D.-W. Li, Z.-W. Ren, H.-X. Yi, X.-F. Wang, J.-H. Tong, X. Chen, B.-J. Zhao, W.-L. Wang, S.-T. Li, J. Mater. Sci.: Mater. Electron. **25**, 4200 (2014)
22. W.C. Peng, Y.C.S. Wu, Appl. Phys. Lett. **88**, 181117 (2006)
23. C.-F. Lin, C.-M. Lin, K.-T. Chen, W.-C. Huang, M.-S. Lin, J.-J. Dai, R.-H. Jiang, Y.-C. Huang, C.-Y. Chang, Appl. Phys. Lett. **95**, 201102 (2009)
24. W.C. Peng, Y.C.S. Wu, Jpn. J. Appl. Phys. **45**, 7709 (2006)
25. Y.M. Song, E.S. Choi, G.C. Park, C.Y. Park, S.J. Jang, Y.T. Lee, Appl. Phys. Lett. **97**, 093110 (2010)
26. S.-M. Pan, R.-C. Tu, Y.-M. Fan, R.-C. Yeh, J.-T. Hsu, IEEE Photonics Technol. Lett. **15**, 649 (2003)
27. T. Fujii, Y. Gao, R. Sharma, E.L. Hu, S.P. DenBaars, S. Nakamura, Appl. Phys. Lett. **84**, 856 (2004)
28. H.-S. Kwack, H.S. Lim, H.-D. Song, S.-H. Jung, H.K. Cho, H.-K. Kwon, M.S. Oh, AIP Adv. **2**, 022127 (2012)
29. C.-C. Kao, H.C. Kuo, K.F. Yeh, J.T. Chu, W.L. Peng, H.W. Huang, T.C. Lu, S.C. Wang, IEEE Photonics Technol. Lett. **19**, 849 (2007)
30. C.-E. Lee, Y.-C. Lee, H.-C. Kuo, T.-C. Lu, S.-C. Wang, IEEE Photonics Technol. Lett. **20**, 803 (2008)
31. Wei-Chi Lee, Shui-Jinn Wang, Kai-Ming Uang, Tron-Min Chen, Der-Ming Kuo, Pei-Ren Wang, Po-Hong Wang, IEEE Photonics Technol. Lett. **22**, 1318 (2010)
32. Y.-J. Lee, H.-C. Kuo, T.-C. Lu, S.-C. Wang, IEEE J. Quantum Electron. **42**, 1196 (2006)
33. D. Zhuang, J.H. Edgar, Mater. Sci. Eng., R **48**, 1 (2005)
34. T. Hino, S. Tomiya, T. Miyajima, K. Yanashima, S. Hashimoto, M. Ikeda, Appl. Phys. Lett. **76**, 3421 (2000)
35. J.L. Weyher, P.D. Brown, J.L. Rouviere, T. Wosinski, A.R.A. Zauner, I. Grzegory, J. Cryst. Growth **210**, 151 (2000)